

# Debias-DAPO: Mitigating Unimodal Bias in Multi-modal Large Language Models via Attention-Based Reward and Modality-Balanced Learning

Anonymous CVPR submission

Paper ID \*\*\*\*\*

## Abstract

Multi-modal Large Language Models (MLLMs) have made significant progress in various applications but still suffer from unimodal bias, particularly "textual supremacy and visual neglect," leading to multimodal hallucinations. To address this challenge, we propose an enhancement to the DAPO algorithm, Debias-DAPO, which introduces attention-anchored hard negative mining and preference-shaping term that operates only over high-quality responses to correct answers that excessively rely on text. By calculating the ratio of per-token attention between text and visual modalities, we quantify unimodal bias. The reward function incentivizes responses grounded in vision while penalizing excessive text dependence, directly addressing harmful text biases. Meanwhile, by token-weighted advantage distribution using attention-derived evidence weights, optimization is refocused on key output tokens grounded in visual evidence. This ensures gradient updates prioritize visual information, encouraging the model to base its reasoning on images. Additionally, we introduce the first modality-balanced dataset, designed to overcome limitations in existing multimodal datasets. This dataset includes multimodal data where the multimodal response is correct, but unimodal responses are incorrect, along with manually verified contradictory image-text pairs and Chain of Thought (CoT) data. The goal is to encourage models to reason using both modalities effectively. Extensive experiments validate Debias-DAPO, demonstrating that it maintains visual grounding while effectively suppressing text bias drift, outperforming strong DAPO baselines. B

## 1. Introduction

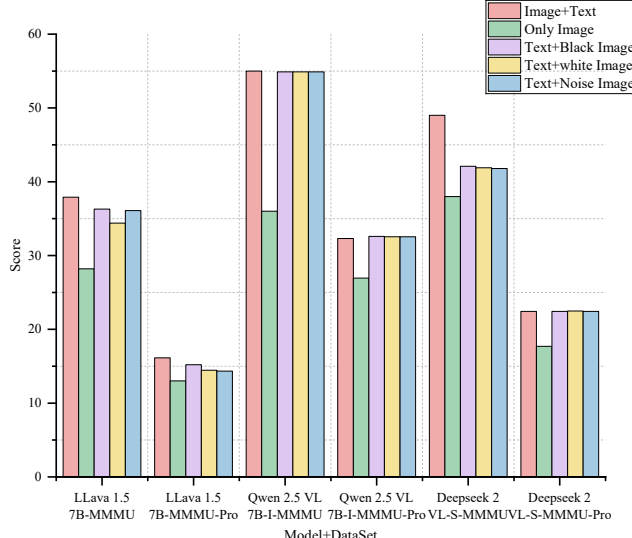
Recent advancements in Multimodal Large Language Models (MLLMs) have led to significant progress across various tasks [? ]. By integrating multiple modalities, such as text, audio, and images, these models have proven effective across diverse domains. However, a persistent chal-

lenge remains: MLLMs often exhibit unimodal bias, favoring one modality—typically text—while neglecting others. This bias can lead to over-reliance on a single modality, causing the model to generate responses that seem confident but are inaccurate or biased when information from less dominant modalities is missing or incorrect.

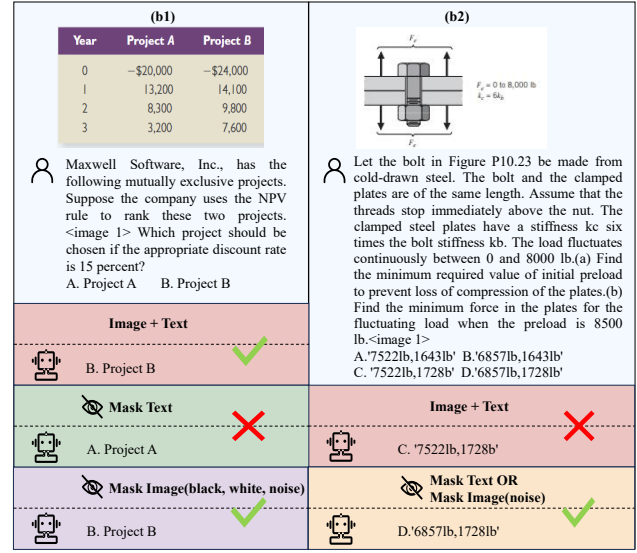
As illustrated in Fig. ??(a), MLLMs commonly demonstrate uneven reliance on input modalities, with a clear text-dominant bias. For example, models like LLaVA ([11]), Qwen-VL ([2]), and DeepSeek-VL ([26]) produce correct answers with text-image inputs, but fail when only visual inputs are provided. In more extreme cases, models generate incorrect answers with text-image pairs but succeed with text-only inputs, ignoring the visual modality entirely (Fig. ??(b2)). This paradox underscores the issue: the model relies excessively on text, sidelining visual information even when it is crucial for accuracy. These biases prevent the model from fully exploiting multimodal information and lead to overconfident errors when non-dominant modalities are absent or degraded. The ideal MLLM should integrate information from all modalities to ensure robust, accurate responses in a variety of conditions.

To mitigate this issue, existing approaches have attempted to balance modality usage by altering dataset distributions [32], applying causal interventions [3], and debiasing during training [16]. However, these solutions often require large-scale supervised fine-tuning and show limited generalization. To address these limitations, we introduce the \*\*first dedicated unimodal bias dataset\*\*, designed to address current benchmarks' shortcomings and facilitate better multimodal integration.

Building on existing datasets like A-OKVQA [20], VisRAG-Ret-Test-ArxivQA [27], and TextVQA [22], we develop a novel data construction methodology. Our approach introduces modal conflicts by perturbing complementary modalities, forcing models to reason effectively in scenarios involving unimodal bias and conflict. The resulting \*\*Debiased Multimodal Dataset\*\* includes two crucial subsets: multimodal correct data and modality-conflicting samples. The multimodal correct subset retains only sam-



(a) Dataset vs. accuracy



(b) Ablation study

Figure 1. Overall caption for the two panels.

076    ples that require simultaneous use of both text and image  
077    information to generate correct answers. The modality-  
078    conflicting subset consists of data where the visual and tex-  
079    tual information contradict each other, manually verified for  
080    quality.

081    To further tackle unimodal bias, we extend the DAPO  
082    framework ([? ]) by introducing a bias-specific reward  
083    function. This reward function integrates modality-balance  
084    and task-accuracy rewards, encouraging models to focus on  
085    both visual and textual information. Additionally, we intro-  
086    duce \*\*Chain-of-Thought (CoT)\*\* reasoning to guide the  
087    model’s stepwise decision-making, improving robustness in  
088    challenging tasks.

089    We evaluate our approach using models such as  
090    Qwen2.5-VL-7B-Instruct [2], LLaVA-1.5 [11], and  
091    DeepSeek-VL2-small [26]. We train the models using the  
092    generated Debiased Multimodal Dataset and assess perfor-  
093    mance on both VLind-Bench [9] and standard hallucination  
094    benchmarks, including MMHalBench [23], AMBER [24],  
095    and CHAIR [18]. Our method significantly outperforms  
096    baseline models like NAPO ([29]) in terms of accuracy and  
097    hallucination reduction, demonstrating the effectiveness of  
098    the \*\*Debiased Multimodal Dataset\*\* and the enhanced  
099    DAPO algorithm.

## 100    2. Related work

### 101    2.1. Unimodal bias in MLLMs

102    In recent years, significant advancements have been made  
103    in MLLMs([6],[4],[8]). Unimodal bias occurs when mod-  
104    els prioritize simple patterns within a single modality while  
105    neglecting the strengths of other modalities, leading to per-

106    formance degradation and hallucinations when modalities  
107    are missing during inference [33]. For instance, prompt  
108    text significantly influences the performance of many state-  
109    of-the-art multimodal models. Model performance im-  
110    proves substantially when textual prompts are included,  
111    but degrades drastically without this modality. In re-  
112    cent years, significant advancements have been made in  
113    MLLMs([6],[4],[8]). Unimodal bias occurs when models  
114    prioritize simple patterns within a single modality while ne-  
115    glecting the strengths of other modalities, leading to per-  
116    formance degradation and hallucinations when modalities are  
117    missing during inference [33]. For instance, prompt text  
118    significantly influences the performance of many state-of-  
119    the-art multimodal models. Model performance improves  
120    substantially when textual prompts are included, but de-  
121    grades drastically without this modality. Various methods  
122    have been proposed to quantify and mitigate unimodal bias  
123    in VQA tasks, with a focus on balancing datasets [32] and  
124    complex training strategies [7] [31] [30]. Recent research  
125    includes modality bias evaluation benchmarks [9], datasets  
126    for modality bias [15], weight adjustments [12], prompt-  
127    ing strategies [5], Preference Optimization [31], [30], and  
128    decoding configurations to reduce language priors [14]  
129    [28]. Preference Optimization fine-tunes models with hu-  
130    man feedback to align outputs with human expectations.  
131    Recent work, like Noise-robust Alignment with Prefer-  
132    ence Optimization (NAPO) [29], incorporates noise-robust  
133    mechanisms into the Direct Preference Optimization (DPO)  
134    framework [17], which corrects errors but does not funda-  
135    mentally change the model’s capabilities. The Shortcut-  
136    aware MM-RM algorithm [?] mitigates out-of-distribution

137 generalization deficits caused by over-reliance on unimodal  
 138 textual correlations. *By contrast, we introduce a dataset for*  
 139 *determining whether the modality is balanced, while optimiz-*  
 140 *ing the reward model and sampling mechanism of the*  
 141 *GRPO [21] algorithm to mitigate unimodal bias and hallu-*  
 142 *cination.*

## 143 2.2. MLLMs Post Training with RL

144 Reinforcement learning (RL) develops intelligent agents  
 145 by learning optimal policies through trial-and-error inter-  
 146 actions to maximize rewards. Recently, RL has seen signif-  
 147 icant progress in multimodal large models. Proximal Policy  
 148 Optimization (PPO) ([19]) is a policy-gradient algorithm  
 149 that stabilizes training by constraining policy update mag-  
 150 nitudes. ReMax is an off-policy RL algorithm that opti-  
 151 mizes the policy via a “relative policy improvement” mech-  
 152 anism, avoiding the complex and unstable evaluation steps  
 153 of conventional methods [10]. More recently, Grouped  
 154 Relative Policy Optimization (GRPO) [21] improves pol-  
 155 icy optimization efficiency by using grouped updates and  
 156 relative entropy constraints, reducing repetitive calculations  
 157 and balancing exploration and exploitation. Despite these  
 158 advancements, a critical issue remains: modality imbal-  
 159 ance, which can significantly impact the contribution of  
 160 each modality to the reward function.

## 161 3. Method

### 162 3.1. Preliminary

#### 163 3.1.1. DAPO

164 DAPO (Decoupled Clip and Dynamic Sampling Policy Opti-  
 165 mization) [?] is an open-source reinforcement learning  
 166 system and engineering framework designed to sup-  
 167 port efficient, reproducible, and scalable complex reason-  
 168 ing tasks with large language models (LLMs). The effi-  
 169 cacy of the proposed approach is comparable to or superior  
 170 to conventional methods in terms of performance, whilst  
 171 concomitantly enhancing the efficiency of training and re-  
 172 ducing computational expenses. It is noteworthy that the  
 173 DAPO model outperforms the GRPO model despite utilising  
 174 a mere half of the training steps.

175 While maintaining GRPO’s utilisation of intra-group rel-  
 176 ative rewards and a clipped objective, DAPO incorporates  
 177 four pivotal engineering enhancements: The following tech-  
 178 niques are employed: clip-higher dynamic sampling, token-  
 179 level loss, and overlong reward shaping. The KL penalty  
 180 term is also removed. These innovations effectively address  
 181 several limitations of GRPO, including entropy collapse,  
 182 gradient wastage, and weight dilution in long-horizon rea-  
 183 soning tasks, leading to more stable and efficient training.

184 As a result, DAPO delivers superior performance, ac-  
 185 celerated training convergence, enhanced stability, and im-  
 186 proved reproducibility. Its efficacy has been demonstrated

187 through successful implementation in a range of large-scale  
 188 model deployments [? ]. The objective function of DAPO  
 189 is given by:

$$\begin{aligned} \mathcal{J}_{\text{DAPO}}(\theta) = & \mathbb{E}[(q, a) \sim \mathcal{D}, \{o_i\}_{i=1}^G \sim \pi_{\theta_{\text{old}}}(\cdot | q)] \\ & \left[ \frac{1}{\sum_{i=1}^G |o_i|} \sum_{i=1}^G \sum_{t=1}^{|o_i|} \min \left( r_{i,t}(\theta) \hat{A}_{i,t}, \right. \right. \\ & \left. \left. \text{clip} \left( r_{i,t}(\theta), 1 - \varepsilon_{\text{low}}, 1 + \varepsilon_{\text{high}} \right) \hat{A}_{i,t} \right) \right] \end{aligned} \quad (1) \quad 190$$

$$\text{s.t. } 0 < \left| \{o_i \mid \text{is\_equivalent}(a, o_i)\} \right| < G \quad 191$$

192 where

$$r_{i,t}(\theta) = \frac{\pi_\theta(o_{i,t} \mid q, o_{i,<t})}{\pi_{\theta_{\text{old}}}(o_{i,t} \mid q, o_{i,<t})}, \quad \hat{A}_{i,t} = \frac{R_i - \text{mean}(\{R_i\}_{i=1}^G)}{\text{std}(\{R_i\}_{i=1}^G)} \quad (2) \quad 193$$

194 Randomly sample a question-answer pair ( $q, a$ ) from  
 195 the training dataset  $\mathcal{D}$ . Using the old policy model  
 196  $\pi_{\theta_{\text{old}}}$ , generate a set of  $G$  responses for question  $q$ .  
 $\frac{1}{\sum_{i=1}^G |o_i|} \sum_{i=1}^G \sum_{t=1}^{|o_i|}$  indicates we will compute the loss  
 197 for each token in every response, then normalize by the total  
 198 number of tokens across all responses.  $r_{i,t}$  measures the  
 199 change in token selection probability between the new and  
 200 old policies. The advantage function  $\hat{A}_{i,t}$  measures how  
 201 well the decision to generate this token performs relative to  
 202 the average, given the question and historical context. The  
 203  $\min(r_{i,t}(\theta) \hat{A}_{i,t}, \text{clip}(r_{i,t}(\theta), 1 - \varepsilon_{\text{low}}, 1 + \varepsilon_{\text{high}}) \hat{A}_{i,t})$  op-  
 204 eration decouples and prunes the model. By actively en-  
 205 couraging exploration with a larger upper bound  $\varepsilon_{\text{high}}$  while  
 206 strictly constraining the maximum step size of policy up-  
 207 dates with a more conservative lower bound  $\varepsilon_{\text{low}}$ , it achieves  
 208 a critical balance between improving performance and pre-  
 209 venting training collapse, ensuring the stability of the train-  
 210 ing process.   
 211

#### 212 3.1.2. Reward Function

213 DAPO employs a fully rule-driven reward function, mov-  
 214 ing away from the often unreliable neural network-based  
 215 reward models typically used in traditional reinforce-  
 216 ment learning. The fundamental principle of the method is to  
 217 assign a binary reward of positive one or negative one,  
 218 based solely on the final correctness of the generated an-  
 219 swer. This straightforward reward scheme ensures strong  
 220 alignment between the optimization objective and the task  
 221 goal, effectively circumventing reward hacking. In order  
 222 to regulate the output length, DAPO incorporates an adap-  
 223 tive length penalty mechanism. This mechanism progres-  
 224 sively penalises responses that exceed a predefined thresh-  
 225 old, thereby encouraging the model to generate concise an-  
 226 swers without interfering with valid reasoning processes.

During the forward pass, DAPO deploys a meticulously structured batch sampling and training procedure. For each query, multiple responses are generated dynamically, and sample groups that cannot contribute meaningful gradient signals are filtered out strategically; this may include those that are entirely correct or entirely incorrect. Consequently, it is assured that every parameter update is informed by data of significant value. The advantage for each response is then computed using group-wise reward normalization, thereby eliminating the need for a complex value function. In the subsequent loss computation phase, DAPO employs a novel approach by implementing token-level policy optimisation and utilising decoupled clipping on importance sampling ratios. The amalgamation of these design choices ensures elevated stability and sample efficiency throughout the course of large-scale reinforcement learning training.

## 3.2. Debiased Multimodal Datasets

### 3.2.1. Overview

In this paper, we propose the first open-source resource designed dataset for achieving modality balance, namely Debiased Multi-Modal dataset (**DMM**).

Recent research has revealed that unimodal bias arises from a model’s over-reliance on one modality (textual or visual) while neglecting the other. To address this problem, we focus on enhancing inter-modal correlations and incorporates scenarios where modalities conflict. Extending beyond conventional visual question answering, our DMM dataset includes samples that require both visual and textual information for correct responses — cases that a single modality cannot adequately address. Meanwhile, our DMM dataset introduces conflicting samples where the textual and visual content diverge, thereby establishing a foundation for reward mechanisms based on modal equilibrium.

For each bimodal data sample and its corresponding conflicting sample in the training set, Chain-of-Thought (COT) [25] data is generated using GPT-4.1 [1]. The Debias dataset builds upon A-OKVQA [20], VisRAG-Ret-Test-ArxivQA[27], and TextVQA [22], covering a wide range of topics, including commonsense reasoning, encyclopedic knowledge, diagram interpretation, and physical principles. The dataset is partitioned into training and test sets containing 12,000 and 1,200 visual question–answer pairs respectively. Images are provided in JPG and PNG formats with resolutions ranging from 448 to 1024 pixels. In total, the dataset consists of 13,200 visual question-answer pairs. 91.67% of these represent unbiased examples. The remaining 8.33% comprise modality-conflicting instances.

### 3.2.2. Dataset Construction

#### Data Design for Enhanced Modality Complementarity.

We introduce a filtering process based on the OK-VQA ([13]), A-OKVQA ([20]), VisRAG-Ret-Test-ArxivQA[27]

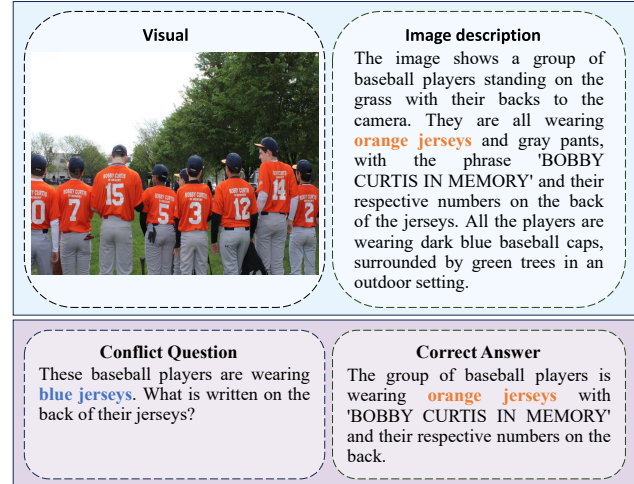


Figure 2. Put your overall caption here.

datasets. First, we utilize the original images and text questions to identify data points with correct answers. Next, we test the model using only the images. The original text questions were replaced with a simple prompt such as ‘Please answer the question based on the image.’ We then tested using only the text. The original images were replaced with black images. This process removed data that could be answered correctly using only one modality (either images or text alone). We specifically target data requiring combined information from both modalities. For example, a text question might ask, ‘Is the rabbit on the chair?’, when the image clearly shows the rabbit on a table. Answering this correctly requires using the image to correct the text’s premise. Ultimately, 3,310 data points resulted from the filtering.

**Modality-Conflict Samples.** Through initial experiments, we observe that the reward mechanism fails to converge due to the input of biased data. This results in the model’s performance fluctuating unpredictably during training. To encourage large multi-modal models to rely more consistently on reliable modalities, we create a specialized set of samples. Based on the TextVQA dataset [22], we employ **GPT 4.1** to generate conflict samples in which the textual questions contradict the visual content. The aim is to enable multi-modal models to detect such inconsistencies through visual cues, allowing them to correct textual misinformation based on visual evidence rather than simply adhering to the text. The visual attributes in these samples are derived solely from objective image information and serve as the ground truth for identifying contradictions. The textual questions are designed to introduce conflicts centered around these samples, including attribute contradictions, object existence conflicts and state or action discrepancies. For instance, for an image showing a group of baseball players standing on the grass, all wearing orange

jerseys with the text 'BOBBY CURTIS IN MEMORY' and their respective numbers on the back, the corresponding question might be: 'These baseball players are wearing blue jerseys. What is written on the back of their jerseys?' A robust model should recognise the discrepancy between the textual reference to 'blue jerseys' and the orange jerseys evident in the image, and respond accurately based on the image. The expected answer would be: 'The group of baseball players is wearing orange jerseys with 'BOBBY CURTIS IN MEMORY' and their respective numbers on the back.' All generated conflict samples are textbf manually verified to ensure that the contradictions could be identified and the answers corrected visually. This process results in a high-quality conflict sample set consisting of 1,000 training samples and 100 test samples.

### 3.3. Debiased Framework

Debias-DAPO augments DAPO with two complementary components: (i) an attention-anchored hard negative mining and preference-shaping term that operates only over high-quality responses, and (ii) token-weighted advantage distribution using attention-derived evidence weights. We use attention patterns as a heuristic proxy for grounding strength, acknowledging that they reflect correlation rather than causation. The complete training objective combines both components with the base DAPO loss:

$$\mathcal{L}_{\text{total}} = \mathcal{L}_{\text{DAPO}}(\theta; \tilde{A}_{i,t}) + \lambda \mathcal{L}_{\text{pref}}(\theta), \quad (3)$$

where  $\mathcal{L}_{\text{DAPO}}$  uses token-weighted advantages  $\tilde{A}_{i,t}$  (Eq. 8) instead of uniform sequence-level advantages, and  $\lambda$  controls the strength of preference regularization.

#### 3.3.1. Attention-Anchored Hard Negative Mining and Preference-Shaping Term

**Visual Grounding Ratio** During rollout generation, we compute a Visual Grounding Ratio (VGR) using all layers and heads while filtering out special/system tokens (BOS, system/role markers, PAD/EOS), so the prompt side contains only visual tokens ( $V$ ) and question tokens ( $T$ ). For each layer-head  $(\ell, h)$ , take the generation  $\times$  prompt attention slice and row-normalize it within  $(V \cup T)$ :  $\tilde{\alpha}_{t \rightarrow k}^{(\ell,h)} = \alpha_{t \rightarrow k}^{(\ell,h)} / \sum_{k' \in V \cup T} \alpha_{t \rightarrow k'}^{(\ell,h)}$ . Let  $G$  be the set of generated tokens. We aggregate across all  $(\ell, h, t)$  compactly via a mean operator to obtain modality masses:

$$\hat{A}_V = \text{mean}_{\ell,h,t} \left( \sum_{k \in V} \tilde{\alpha}_{t \rightarrow k}^{(\ell,h)} \right), \quad \hat{A}_T = \text{mean}_{\ell,h,t} \left( \sum_{k \in T} \tilde{\alpha}_{t \rightarrow k}^{(\ell,h)} \right), \quad (4)$$

and define the VGR by normalizing with token counts:

$$\text{VGR} = \frac{\hat{A}_V / |V|}{\hat{A}_T / |T|}. \quad (5)$$

To reduce confounds from sequence length and question difficulty, we apply a **per-question monotone normalization** to raw VGR scores. Specifically, within each question's response group (the  $G$  responses generated for that question), we apply rank-based quantile transformation to map VGR values to a standard distribution, producing the normalized score  $s_i$  used in Eq. 6. This monotone transformation preserves the relative ordering of responses while controlling for question-specific variations in attention patterns.

**Within-positive preference shaping.** Within each question's high-quality response set  $\mathcal{P} = \{y_i\}$  (responses receiving positive rewards in DAPO's rule-based reward function, i.e., correct answers with valid formatting), we use the group-normalized VGR score  $s_i$  to identify text-biased positives as hard negatives and to enforce a margin that favors vision-grounded positives—without relabeling. *While these responses are correct in terms of final answers, they are undesirable from a grounding perspective—achieving accuracy through textual shortcuts rather than genuine multimodal reasoning. We thus treat them as negatives in the preference ranking to discourage shortcut learning.* Concretely, we form ordered pairs by sampling (i) from the top- $K$  highest  $s$  (more vision-grounded) and (j) from the bottom- $K$  lowest  $s$  (more text-biased), and optimize a pairwise logistic-margin loss:

$$\mathcal{L}_{\text{pref}} = \mathbb{E}_{(i,j) \sim \mathcal{M}(\mathcal{P})} \left[ -\log \sigma \left( \beta ((s_i - s_j) - m) \right) \right], \quad (6)$$

where  $\mathcal{M}(\mathcal{P})$  denotes the within-positive pairing policy,  $m \geq 0$  is a margin, and  $\beta$  is a temperature. This attention-anchored hard-negative preference-shaping term operates only within high-quality responses, complements the base DAPO objective, and directly suppresses textual shortcuts by ensuring that vision-grounded positives consistently outrank text-biased ones. (An optional listwise variant uses  $\tilde{p}_i = \exp(\lambda s_i) / \sum_{y \in \mathcal{P}} \exp(\lambda s_y)$  as a soft target and minimizes cross-entropy against the policy over  $\mathcal{P}$ .)

#### 3.3.2. Token-Weighted Advantage Distribution using Attention-Derived Evidence Weights

To further refine gradient allocation, we distribute the sequence-level advantage  $\hat{A}_i$  obtained from DAPO to individual output tokens according to normalized attention-derived evidence weights. For each generated token  $t$ , we compute an attention-based evidence weight using the row-normalized attention  $\tilde{\alpha}_{t \rightarrow k}$  (averaged across layers and heads) that measures its grounding in the visual context:

$$w_{i,t} = \frac{\sum_{k \in V} \tilde{\alpha}_{t \rightarrow k}}{\sum_{k \in V \cup T} \tilde{\alpha}_{t \rightarrow k}}, \quad (7)$$

where  $\bar{\alpha}_{t \rightarrow k} = \frac{1}{LH} \sum_{\ell,h} \tilde{\alpha}_{t \rightarrow k}^{(\ell,h)}$  denotes the layer-head averaged normalized attention from token  $t$  to prompt token

404        *k*. These weights are normalized within each sequence:

405        
$$\tilde{A}_{i,t} = \frac{w_{i,t}}{\sum_{t'} w_{i,t'}} \cdot \hat{A}_i. \quad (8)$$

406        The two-stage normalization serves distinct purposes:  $w_{i,t}$   
 407        in Eq. 7 measures each token’s proportional reliance on  
 408        visual context relative to all prompt tokens, while the  
 409        sequence-level renormalization in Eq. 8 ensures that token-  
 410        level advantages sum to the original sequence advan-  
 411        tage  $\hat{A}_i$ , preserving DAPO’s advantage scaling proper-  
 412        ties. This token-weighted advantage distribution routes  
 413        gradients toward evidence-bearing tokens that contribute to  
 414        grounded reasoning, enhancing fine-grained credit assign-  
 415        ment and complementing the within-positive preference-  
 416        shaping term.

## 417        4. Experiments

### 418        4.1. Datasets

### 419        4.2. Training Details

## 420        References

- 421 [1] Josh Achiam, Steven Adler, Sandhini Agarwal, Lama Ah-  
 422 mad, Ilge Akkaya, Florencia Leoni Aleman, Diogo Almeida,  
 423 Janko Altenschmidt, Sam Altman, Shyamal Anadkat, et al.  
 424 Gpt-4 technical report. *arXiv preprint arXiv:2303.08774*,  
 425 2023. 4
- 426 [2] Shuai Bai, Keqin Chen, Xuejing Liu, Jialin Wang, Wenbin  
 427 Ge, Sibo Song, Kai Dang, Peng Wang, Shijie Wang, Jun  
 428 Tang, Humen Zhong, Yuanzhi Zhu, Mingkun Yang, Zhao-  
 429 hai Li, Jianqiang Wan, Pengfei Wang, Wei Ding, Zheren Fu,  
 430 Yiheng Xu, Jiabo Ye, Xi Zhang, Tianbao Xie, Zesen Cheng,  
 431 Hang Zhang, Zhibo Yang, Haiyang Xu, and Junyang Lin.  
 432 Qwen2.5-vl technical report, 2025. 1, 2
- 433 [3] Meiqi Chen, Yixin Cao, Yan Zhang, and Chaochao Lu.  
 434 Quantifying and mitigating unimodal biases in multimodal  
 435 large language models: A causal perspective, 2024. 1
- 436 [4] Zhe Chen, Jiannan Wu, Wenhui Wang, Weijie Su, Guo Chen,  
 437 Sen Xing, Muyan Zhong, Qinglong Zhang, Xizhou Zhu,  
 438 Lewei Lu, Bin Li, Ping Luo, Tong Lu, Yu Qiao, and Jifeng  
 439 Dai. Internvl: Scaling up vision foundation models and  
 440 aligning for generic visual-linguistic tasks, 2024. 2
- 441 [5] Yusheng Dai, Hang Chen, Jun Du, Ruoyu Wang, Shihao  
 442 Chen, Haotian Wang, and Chin-Hui Lee. A study of dropout-  
 443 induced modality bias on robustness to missing video frames  
 444 for audio-visual speech recognition. In *Proceedings of*  
 445 *the IEEE/CVF Conference on Computer Vision and Pattern*  
 446 *Recognition*, pages 27445–27455, 2024. 2
- 447 [6] DeepSeek-AI, Daya Guo, Dejian Yang, Huawei Zhang,  
 448 Junxiao Song, Ruoyu Zhang, Runxin Xu, Qihao Zhu, Shi-  
 449 rong Ma, Peiyi Wang, Xiao Bi, Xiaokang Zhang, Xingkai  
 450 Yu, Yu Wu, Z. F. Wu, Zhibin Gou, Zhihong Shao, Zhuoshu  
 451 Li, Ziyi Gao, Aixin Liu, Bing Xue, Bingxuan Wang, Bochao  
 452 Wu, Bei Feng, Chengda Lu, Chenggang Zhao, Chengqi  
 453 Deng, Chenyu Zhang, Chong Ruan, Damai Dai, Deli Chen,
- 454 Dongjie Ji, Erhang Li, Fangyun Lin, Fucong Dai, Fuli Luo,  
 455 Guangbo Hao, Guanting Chen, Guowei Li, H. Zhang, Han  
 456 Bao, Hanwei Xu, Haocheng Wang, Honghui Ding, Huajian  
 457 Xin, Huazuo Gao, Hui Qu, Hui Li, Jianzhong Guo, Jiashi Li,  
 458 Jiawei Wang, Jingchang Chen, Jingyang Yuan, Junjie Qiu,  
 459 Junlong Li, J. L. Cai, Jiaqi Ni, Jian Liang, Jin Chen, Kai  
 460 Dong, Kai Hu, Kaige Gao, Kang Guan, Kexin Huang, Kuai  
 461 Yu, Lean Wang, Lecong Zhang, Liang Zhao, Litong Wang,  
 462 Liyue Zhang, Lei Xu, Leyi Xia, Mingchuan Zhang, Minghua  
 463 Zhang, Minghui Tang, Meng Li, Miaojun Wang, Ming-  
 464 ming Li, Ning Tian, Panpan Huang, Peng Zhang, Qiancheng  
 465 Wang, Qinyu Chen, Qiushi Du, Ruiqi Ge, Ruisong Zhang,  
 466 Ruizhe Pan, Runji Wang, R. J. Chen, R. L. Jin, Ruyi Chen,  
 467 Shanghao Lu, Shangyan Zhou, Shanhua Chen, Shengfeng  
 468 Ye, Shiyu Wang, Shuiping Yu, Shunfeng Zhou, Shuting Pan,  
 469 S. S. Li, Shuang Zhou, Shaoqing Wu, Shengfeng Ye, Tao  
 470 Yun, Tian Pei, Tianyu Sun, T. Wang, Wangding Zeng, Wan-  
 471 jia Zhao, Wen Liu, Wenfeng Liang, Wenjun Gao, Wenqin Yu,  
 472 Wentao Zhang, W. L. Xiao, Wei An, Xiaodong Liu, Xiaohan  
 473 Wang, Xiaokang Chen, Xiaotao Nie, Xin Cheng, Xin Liu,  
 474 Xin Xie, Xingchao Liu, Xinyu Yang, Xinyuan Li, Xuecheng  
 475 Su, Xuheng Lin, X. Q. Li, Xiangyu Jin, Xiaojin Shen, Xi-  
 476 aoshua Chen, Xiaowen Sun, Xiaoxiang Wang, Xinnan Song,  
 477 Xinyi Zhou, Xianzu Wang, Xinxia Shan, Y. K. Li, Y. Q.  
 478 Wang, Y. X. Wei, Yang Zhang, Yanhong Xu, Yao Li, Yao  
 479 Zhao, Yaofeng Sun, Yaohui Wang, Yi Yu, Yichao Zhang, Yi-  
 480 fan Shi, Yiliang Xiong, Ying He, Yishi Piao, Yisong Wang,  
 481 Yixuan Tan, Yiyang Ma, Yiyuan Liu, Yongqiang Guo, Yuan  
 482 Ou, Yuduan Wang, Yue Gong, Yuheng Zou, Yujia He, Yun-  
 483 fan Xiong, Yuxiang Luo, Yuxiang You, Yuxuan Liu, Yuyang  
 484 Zhou, Y. X. Zhu, Yanhong Xu, Yanping Huang, Yaohui Li,  
 485 Yi Zheng, Yuchen Zhu, Yunxian Ma, Ying Tang, Yukun  
 486 Zha, Yuting Yan, Z. Z. Ren, Zehui Ren, Zhangli Sha, Zhe  
 487 Fu, Zhean Xu, Zhenda Xie, Zhengyan Zhang, Zhewen Hao,  
 488 Zhicheng Ma, Zhigang Yan, Zhiyu Wu, Zihui Gu, Zijia Zhu,  
 489 Zijun Liu, Zilin Li, Ziwei Xie, Ziyang Song, Zizheng Pan,  
 490 Zhen Huang, Zhipeng Xu, Zhongyu Zhang, and Zhen Zhang.  
 491 Deepseek-r1: Incentivizing reasoning capability in llms via  
 492 reinforcement learning, 2025. 2
- 493 [7] Yunfeng Fan, Wenchao Xu, Haozhao Wang, Fushuo Huo,  
 494 Jinyu Chen, and Song Guo. Overcome modal bias in multi-  
 495 modal federated learning via balanced modality selection. In  
 496 *European Conference on Computer Vision*, pages 178–195.  
 497 Springer, 2024. 2
- 498 [8] Aaron Grattafiori, Abhimanyu Dubey, Abhinav Jauhri, Ab-  
 499 hinav Pandey, Abhishek Kadian, Ahmad Al-Dahle, Aiesha  
 500 Letman, Akhil Mathur, Alan Schelten, Alex Vaughan, Amy  
 501 Yang, Angela Fan, Anirudh Goyal, Anthony Hartshorn,  
 502 Aobo Yang, Archi Mitra, Archie Sravankumar, Artem Ko-  
 503 renev, Arthur Hinsvark, Arun Rao, Aston Zhang, Aure-  
 504 lien Rodriguez, Austen Gregerson, Ava Spataru, Baptiste  
 505 Roziere, Bethany Biron, Binh Tang, Bobbie Chern, Charlotte  
 506 Caucheteux, Chaya Nayak, Chloe Bi, Chris Marra, Chris  
 507 McConnell, Christian Keller, Christophe Touret, Chunyang  
 508 Wu, Corinne Wong, Cristian Canton Ferrer, Cyrus Niko-  
 509 laidis, Damien Allonsius, Daniel Song, Danielle Pintz,  
 510 Danny Livshits, Danny Wyatt, David Esiobu, Dhruv Choud-  
 511 hary, Dhruv Mahajan, Diego Garcia-Olano, Diego Perino,

512 Dieuwke Hupkes, Egor Lakomkin, Ehab AlBadawy, Elina  
 513 Lobanova, Emily Dinan, Eric Michael Smith, Filip Raden-  
 514 ovic, Francisco Guzmán, Frank Zhang, Gabriel Synnaeve,  
 515 Gabrielle Lee, Georgia Lewis Anderson, Govind Thattai,  
 516 Graeme Nail, Gregoire Mialon, Guan Pang, Guillem Cu-  
 517 curell, Hailey Nguyen, Hannah Korevaar, Hu Xu, Hugo Tou-  
 518 vron, Iliyan Zarov, Imanol Arrieta Ibarra, Isabel Kloumann,  
 519 Ishan Misra, Ivan Evtimov, Jack Zhang, Jade Copet, Jae-  
 520 won Lee, Jan Geffert, Jana Vranes, Jason Park, Jay Ma-  
 521 hadeokar, Jeet Shah, Jelmer van der Linde, Jennifer Bil-  
 522 lock, Jenny Hong, Jenya Lee, Jeremy Fu, Jianfeng Chi,  
 523 Jianyu Huang, Jiawen Liu, Jie Wang, Jiecao Yu, Joanna Bit-  
 524 ton, Joe Spisak, Jongsoo Park, Joseph Rocca, Joshua John-  
 525 stun, Joshua Saxe, Junteng Jia, Kalyan Vasuden Alwala,  
 526 Karthik Prasad, Kartikeya Upasani, Kate Plawiak, Ke Li,  
 527 Kenneth Heafield, Kevin Stone, Khalid El-Arini, Krithika  
 528 Iyer, Kshitiz Malik, Kuenley Chiu, Kunal Bhalla, Kushal  
 529 Lakhotia, Lauren Rantala-Yeary, Laurens van der Maaten,  
 530 Lawrence Chen, Liang Tan, Liz Jenkins, Louis Martin, Lo-  
 531 vish Madaan, Lubo Malo, Lukas Blecher, Lukas Landzaat,  
 532 Luke de Oliveira, Madeline Muzzi, Mahesh Pasupuleti,  
 533 Mannat Singh, Manohar Paluri, Marcin Kardas, Maria Tsim-  
 534 poukelli, Mathew Oldham, Mathieu Rita, Maya Pavlova,  
 535 Melanie Kambadur, Mike Lewis, Min Si, Mitesh Kumar  
 536 Singh, Mona Hassan, Naman Goyal, Narjes Torabi, Nikolay  
 537 Bashlykov, Nikolay Bogoychev, Niladri Chatterji, Ning  
 538 Zhang, Olivier Duchenne, Onur Çelebi, Patrick Alrassy,  
 539 Pengchuan Zhang, Pengwei Li, Petar Vasic, Peter Weng, Pra-  
 540 jjwal Bhargava, Pratik Dubal, Praveen Krishnan, Punit Singh  
 541 Koura, Puxin Xu, Qing He, Qingxiao Dong, Ragavan Srinivasan,  
 542 Raj Ganapathy, Ramon Calderer, Ricardo Silveira  
 543 Cabral, Robert Stojnic, Roberta Raileanu, Rohan Mah-  
 544 eswari, Rohit Girdhar, Rohit Patel, Romain Sauvestre, Ron-  
 545 nie Polidoro, Roshan Sumbaly, Ross Taylor, Ruan Silva,  
 546 Rui Hou, Rui Wang, Saghar Hosseini, Sahana Chennabasappa,  
 547 Sanjay Singh, Sean Bell, Seohyun Sonia Kim, Sergey Edunov,  
 548 Shaoliang Nie, Sharan Narang, Sharath Rappa, Sheng Shen,  
 549 Shengye Wan, Shruti Bhosale, Shun Zhang, Simon Vandenhende,  
 550 Soumya Batra, Spencer Whitman, Sten Sootla, Stephane Collot,  
 551 Suchin Gururangan, Sydney Borodinsky, Tamar Herman, Tara Fowler,  
 552 Tarek Sheasha, Thomas Georgiou, Thomas Scialom, Tobias Speck-  
 553 bacher, Todor Mihaylov, Tong Xiao, Ujjwal Karn, Vedanuj  
 554 Goswami, Vibhor Gupta, Vignesh Ramanathan, Viktor  
 555 Kerkez, Vincent Gonguet, Virginie Do, Vish Vogeti, Vitor  
 556 Albiero, Vladan Petrovic, Weiwei Chu, Wenhan Xiong,  
 557 Wenyin Fu, Whitney Meers, Xavier Martinet, Xiaodong  
 558 Wang, Xiaofang Wang, Xiaoqing Ellen Tan, Xide Xia, Xin-  
 559 feng Xie, Xuchao Jia, Xuewei Wang, Yaelle Goldschlag,  
 560 Yashesh Gaur, Yasmine Babaei, Yi Wen, Yiwen Song,  
 561 Yuchen Zhang, Yue Li, Yuning Mao, Zacharie Delpierre  
 562 Coudert, Zheng Yan, Zhengxing Chen, Zoe Papakipos, Aad-  
 563 itya Singh, Aayushi Srivastava, Abha Jain, Adam Kelsey,  
 564 Adam Shajnfeld, Adithya Gangidi, Adolfo Victoria, Ahuva  
 565 Goldstand, Ajay Menon, Ajay Sharma, Alex Boesenberg,  
 566 Alexei Baevski, Allie Feinstein, Amanda Kallet, Amit San-  
 567 gani, Amos Teo, Anam Yunus, Andrei Lupu, Andres Al-  
 568 varado, Andrew Caples, Andrew Gu, Andrew Ho, An-

569 drew Poulton, Andrew Ryan, Ankit Ramchandani, Annie  
 570 Dong, Annie Franco, Anuj Goyal, Aparajita Saraf, Arka-  
 571 bandhu Chowdhury, Ashley Gabriel, Ashwin Bharambe, As-  
 572 saf Eisenman, Azadeh Yazdan, Beau James, Ben Maurer,  
 573 Benjamin Leonhardi, Bernie Huang, Beth Loyd, Beto De  
 574 Paola, Bhargavi Paranjape, Bing Liu, Bo Wu, Boyu Ni,  
 575 Braden Hancock, Bram Wasti, Brandon Spence, Brani Sto-  
 576 jkovic, Brian Gamido, Britt Montalvo, Carl Parker, Carly  
 577 Burton, Catalina Mejia, Ce Liu, Changhan Wang, Changkyu  
 578 Kim, Chao Zhou, Chester Hu, Ching-Hsiang Chu, Chris Cai,  
 579 Chris Tindal, Christoph Feichtenhofer, Cynthia Gao, Da-  
 580 mon Civin, Dana Beaty, Daniel Kreymer, Daniel Li, David  
 581 Adkins, David Xu, Davide Testuggine, Delia David, Devi  
 582 Parikh, Diana Liskovich, Didem Foss, Dingkang Wang, Duc  
 583 Le, Dustin Holland, Edward Dowling, Eissa Jamil, Elaine  
 584 Montgomery, Eleonora Presani, Emily Hahn, Emily Wood,  
 585 Eric-Tuan Le, Erik Brinkman, Esteban Arcaute, Evan Dun-  
 586 bar, Evan Smothers, Fei Sun, Felix Kreuk, Feng Tian, Fil-  
 587 ippos Kokkinos, Firat Ozgenel, Francesco Caggioni, Frank  
 588 Kanayet, Frank Seide, Gabriela Medina Florez, Gabriella  
 589 Schwarz, Gada Badeer, Georgia Swee, Gil Halpern, Grant  
 590 Herman, Grigory Sizov, Guangyi, Zhang, Guna Lakshmi-  
 591 narayanan, Hakan Inan, Hamid Shojaanazeri, Han Zou, Han-  
 592 nah Wang, Hanwen Zha, Haroun Habeeb, Harrison Rudolph,  
 593 Helen Suk, Henry Aspegren, Hunter Goldman, Hongyuan  
 594 Zhan, Ibrahim Damlaj, Igor Molybog, Igor Tufanov, Ilias  
 595 Leontiadis, Irina-Elena Veliche, Itai Gat, Jake Weissman,  
 596 James Geboski, James Kohli, Janice Lam, Japhet Asher,  
 597 Jean-Baptiste Gaya, Jeff Marcus, Jeff Tang, Jennifer Chan,  
 598 Jenny Zhen, Jeremy Reizenstein, Jeremy Teboul, Jessica  
 599 Zhong, Jian Jin, Jingyi Yang, Joe Cummings, Jon Carvill,  
 600 Jon Shepard, Jonathan McPhie, Jonathan Torres, Josh Gins-  
 601 burg, Junjie Wang, Kai Wu, Kam Hou U, Karan Saxena,  
 602 Kartikay Khandelwal, Katayoun Zand, Kathy Matosich,  
 603 Kaushik Veeraraghavan, Kelly Michelena, Keqian Li, Kiran  
 604 Jagadeesh, Kun Huang, Kunal Chawla, Kyle Huang, Lailin  
 605 Chen, Lakshya Garg, Lavender A, Leandro Silva, Lee Bell,  
 606 Lei Zhang, Liangpeng Guo, Licheng Yu, Liron Moshkovich,  
 607 Luca Wehrstedt, Madian Khabsa, Manav Avalani, Manish  
 608 Bhatt, Martynas Mankus, Matan Hasson, Matthew Lennie,  
 609 Matthias Reso, Maxim Groshev, Maxim Naumov, Maya  
 610 Lathi, Meghan Keneally, Miao Liu, Michael L. Seltzer,  
 611 Michal Valko, Michelle Restrepo, Mihir Patel, Mik Vy-  
 612 atskov, Mikayel Samvelyan, Mike Clark, Mike Macey, Mike  
 613 Wang, Miquel Jubert Hermoso, Mo Metanat, Mohammad  
 614 Rastegari, Munish Bansal, Nandhini Santhanam, Natascha  
 615 Parks, Natasha White, Navyata Bawa, Nayan Singhal, Nick  
 616 Egebo, Nicolas Usunier, Nikhil Mehta, Nikolay Pavlovich  
 617 Laptev, Ning Dong, Norman Cheng, Oleg Chernoguz, Olivia  
 618 Hart, Omkar Salpekar, Ozlem Kalinli, Parkin Kent, Parth  
 619 Parekh, Paul Saab, Pavan Balaji, Pedro Rittner, Philip Bon-  
 620 trager, Pierre Roux, Piotr Dollar, Polina Zvyagina, Prashant  
 621 Ratanchandani, Pritish Yuvraj, Qian Liang, Rachad Alao,  
 622 Rachel Rodriguez, Rafi Ayub, Raghatham Murthy, Raghu  
 623 Nayani, Rahul Mitra, Rangaprabhu Parthasarathy, Raymond  
 624 Li, Rebekkah Hogan, Robin Battey, Rocky Wang, Russ  
 625 Howes, Ruty Rinott, Sachin Mehta, Sachin Siby, Sai Jayesh  
 626 Bondu, Samyak Datta, Sara Chugh, Sara Hunt, Sargun  
 627

- 628 Dhillon, Sasha Sidorov, Satadru Pan, Saurabh Mahajan,  
 629 Saurabh Verma, Seiji Yamamoto, Sharadh Ramaswamy,  
 630 Shaun Lindsay, Shaun Lindsay, Sheng Feng, Shenghao Lin,  
 631 Shengxin Cindy Zha, Shishir Patil, Shiva Shankar, Shuqiang  
 632 Zhang, Shuqiang Zhang, Sinong Wang, Sneha Agarwal, Soji  
 633 Sajuyigbe, Soumith Chintala, Stephanie Max, Stephen Chen,  
 634 Steve Kehoe, Steve Satterfield, Sudarshan Govindaprasad,  
 635 Sumit Gupta, Summer Deng, Sungmin Cho, Sunny Virk,  
 636 Suraj Subramanian, Sy Choudhury, Sydney Goldman, Tal  
 637 Remez, Tamar Glaser, Tamara Best, Thilo Koehler, Thomas  
 638 Robinson, Tianhe Li, Tianjun Zhang, Tim Matthews, Timothy  
 639 Chou, Tzook Shaked, Varun Vontimitta, Victoria Ajayi,  
 640 Victoria Montanez, Vijai Mohan, Vinay Satish Kumar,  
 641 Vishal Mangla, Vlad Ionescu, Vlad Poenaru, Vlad Tiberiu  
 642 Mihailescu, Vladimir Ivanov, Wei Li, Wencheng Wang, Wen-  
 643 wen Jiang, Wes Bouaziz, Will Constable, Xiaocheng Tang,  
 644 Xiaoqian Wu, Xiaolan Wang, Xilun Wu, Xinbo Gao, Yaniv  
 645 Kleinman, Yanjun Chen, Ye Hu, Ye Jia, Ye Qi, Yenda Li,  
 646 Yilin Zhang, Ying Zhang, Yossi Adi, Youngjin Nam, Yu,  
 647 Wang, Yu Zhao, Yuchen Hao, Yundi Qian, Yunlu Li, Yuzi  
 648 He, Zach Rait, Zachary DeVito, Zef Rosnbrick, Zhaoduo  
 649 Wen, Zhenyu Yang, Zhiwei Zhao, and Zhiyu Ma. The llama  
 650 3 herd of models, 2024. 2
- [9] Kang il Lee, Minbeom Kim, Seunghyun Yoon, Minsung  
 651 Kim, Dongryeol Lee, Hyukhun Koh, and Kyomin Jung.  
 652 Vlind-bench: Measuring language priors in large vision-  
 653 language models, 2025. 2
- [10] Ziniu Li, Tian Xu, Yushun Zhang, Zhihang Lin, Yang Yu,  
 654 Ruoyu Sun, and Zhi-Quan Luo. Remax: A simple, effec-  
 655 tive, and efficient reinforcement learning method for aligning  
 656 large language models, 2024. 3
- [11] Haotian Liu, Chunyuan Li, Qingyang Wu, and Yong Jae Lee.  
 657 Visual instruction tuning. *Advances in neural information*  
 658 *processing systems*, 36:34892–34916, 2023. 1, 2
- [12] Shi Liu, Kecheng Zheng, and Wei Chen. Paying more at-  
 663 tention to image: A training-free method for alleviating hal-  
 664 lucination in lilm. In *European Conference on Computer*  
 665 *Vision*, pages 125–140. Springer, 2024. 2
- [13] Kenneth Marino, Mohammad Rastegari, Ali Farhadi, and  
 666 Rozbeh Mottaghi. Ok-vqa: A visual question answering  
 667 benchmark requiring external knowledge. In *Proceedings of*  
 668 *the IEEE/CVF Conference on Computer Vision and Pattern*  
 669 *Recognition (CVPR)*, 2019. 4
- [14] Kyungmin Min, Minbeom Kim, Kang-il Lee, Dongryeol  
 672 Lee, and Kyomin Jung. Mitigating hallucinations in  
 673 large vision-language models via summary-guided decoding.  
 674 *arXiv preprint arXiv:2410.13321*, 2024. 2
- [15] Jean Park, Kuk Jin Jang, Basam Alasaly, Sriharsha Mopi-  
 676 devi, Andrew Zolensky, Eric Eaton, Insup Lee, and Kevin  
 677 Johnson. Assessing modality bias in video question answer-  
 678 ing benchmarks with multimodal large language models. In  
 679 *Proceedings of the AAAI Conference on Artificial Intelli-*  
 680 *gence*, pages 19821–19829, 2025. 2
- [16] Vaidehi Patil, Adyasha Maharana, and Mohit Bansal. Debi-  
 682 asing multimodal models via causal information minimization,  
 683 2023. 1
- [17] Rafael Rafailov, Archit Sharma, Eric Mitchell, Christo-  
 684 pher D Manning, Stefano Ermon, and Chelsea Finn. Direct  
 685 preference optimization: Your language model is secretly a  
 686 reward model. *Advances in neural information processing*  
 687 *systems*, 36:53728–53741, 2023. 2
- [18] Anna Rohrbach, Lisa Anne Hendricks, Kaylee Burns, Trevor  
 689 Darrell, and Kate Saenko. Object hallucination in image cap-  
 690 tioning, 2019. 2
- [19] John Schulman, Filip Wolski, Prafulla Dhariwal, Alec Rad-  
 692 ford, and Oleg Klimov. Proximal policy optimization algo-  
 693 rithms. *arXiv preprint arXiv:1707.06347*, 2017. 3
- [20] Dustin Schwenk, Apoorv Khandelwal, Christopher Clark,  
 695 Kenneth Marino, and Roozbeh Mottaghi. A-okvqa: A  
 696 benchmark for visual question answering using world knowl-  
 697 edge. In *European conference on computer vision*, pages  
 698 146–162. Springer, 2022. 1, 4
- [21] Zhihong Shao, Peiyi Wang, Qihao Zhu, Runxin Xu, Junxiao  
 700 Song, Xiao Bi, Haowei Zhang, Mingchuan Zhang, YK Li,  
 701 Yang Wu, et al. Deepseekmath: Pushing the limits of math-  
 702 ematical reasoning in open language models. *arXiv preprint*  
 703 *arXiv:2402.03300*, 2024. 3
- [22] Amanpreet Singh, Vivek Natarajan, Meet Shah, Yu Jiang,  
 705 Xinlei Chen, Dhruv Batra, Devi Parikh, and Marcus  
 706 Rohrbach. Towards vqa models that can read. In *Proceedings*  
 707 *of the IEEE/CVF conference on computer vision and pattern*  
 708 *recognition*, pages 8317–8326, 2019. 1, 4
- [23] Zhiqing Sun, Sheng Shen, Shengcao Cao, Haotian Liu,  
 710 Chunyuan Li, Yikang Shen, Chuang Gan, Liang-Yan Gui,  
 711 Yu-Xiong Wang, Yiming Yang, Kurt Keutzer, and Trevor  
 712 Darrell. Aligning large multimodal models with factually  
 713 augmented rlhf, 2023. 2
- [24] Junyang Wang, Yuhang Wang, Guohai Xu, Jing Zhang,  
 715 Yukai Gu, Haitao Jia, Jiaqi Wang, Haiyang Xu, Ming Yan,  
 716 Ji Zhang, and Jitao Sang. Amber: An llm-free multi-  
 717 dimensional benchmark for mllms hallucination evaluation,  
 718 2024. 2
- [25] Jason Wei, Xuezhi Wang, Dale Schuurmans, Maarten  
 720 Bosma, Fei Xia, Ed Chi, Quoc V Le, Denny Zhou, et al.  
 721 Chain-of-thought prompting elicits reasoning in large lan-  
 722 guage models. *Advances in neural information processing*  
 723 *systems*, 35:24824–24837, 2022. 4
- [26] Zhiyu Wu, Xiaokang Chen, Zizheng Pan, Xingchao Liu,  
 725 Wen Liu, Damai Dai, Huazuo Gao, Yiyang Ma, Chengyue  
 726 Wu, Bingxuan Wang, Zhenda Xie, Yu Wu, Kai Hu, Jiawei  
 727 Wang, Yaofeng Sun, Yukun Li, Yishi Piao, Kang Guan,  
 728 Aixin Liu, Xin Xie, Yuxiang You, Kai Dong, Xingkai Yu,  
 729 Haowei Zhang, Liang Zhao, Yisong Wang, and Chong Ruan.  
 730 Deepseek-vl2: Mixture-of-experts vision-language models  
 731 for advanced multimodal understanding, 2024. 1, 2
- [27] Shi Yu, Chaoyue Tang, Bokai Xu, Junbo Cui, Junhao  
 733 Ran, Yukun Yan, Zhenghao Liu, Shuo Wang, Xu Han,  
 734 Zhiyuan Liu, et al. Visrag: Vision-based retrieval-augmented  
 735 generation on multi-modality documents. *arXiv preprint*  
 736 *arXiv:2410.10594*, 2024. 1, 4
- [28] Yi-Fan Zhang, Weichen Yu, Qingsong Wen, Xue Wang,  
 738 Zhang Zhang, Liang Wang, Rong Jin, and Tieniu Tan. De-  
 739 biasing multimodal large language models. *arXiv preprint*  
 740 *arXiv:2403.05262*, 2024. 2
- [29] Zefeng Zhang, Hengzhu Tang, Jiawei Sheng, Zhenyu Zhang,  
 742 Yiming Ren, Zhenyang Li, Dawei Yin, Duohe Ma, and  
 743

- 744 Tingwen Liu. Debiasing multimodal large language mod-  
745 els via noise-aware preference optimization. In *Proceedings*  
746 *of the Computer Vision and Pattern Recognition Conference*,  
747 pages 9423–9433, 2025. 2
- 748 [30] Xu Zheng, Yuanhuiyi Lyu, and Lin Wang. Learning  
749 modality-agnostic representation for semantic segmentation  
750 from any modalities. In *European Conference on Computer*  
751 *Vision*, pages 146–165. Springer, 2024. 2
- 752 [31] Xu Zheng, Yuanhuiyi Lyu, Jiazhou Zhou, and Lin Wang.  
753 Centering the value of every modality: Towards efficient  
754 and resilient modality-agnostic semantic segmentation. In  
755 *European Conference on Computer Vision*, pages 192–212.  
756 Springer, 2024. 2
- 757 [32] Xu Zheng, Chenfei Liao, Yuqian Fu, Kaiyu Lei, Yuan-  
758 huiyi Lyu, Lutao Jiang, Bin Ren, Jialei Chen, Jiawen Wang,  
759 Chengxin Li, Linfeng Zhang, Danda Pani Paudel, Xuanjing  
760 Huang, Yu-Gang Jiang, Nicu Sebe, Dacheng Tao, Luc Van  
761 Gool, and Xuming Hu. Mllms are deeply affected by modal-  
762 ity bias, 2025. 1, 2
- 763 [33] Xu Zheng, Yuanhuiyi Lyu, Lutao Jiang, Danda Pani Paudel,  
764 Luc Van Gool, and Xuming Hu. Reducing unimodal  
765 bias in multi-modal semantic segmentation with multi-  
766 scale functional entropy regularization. *arXiv preprint*  
767 *arXiv:2505.06635*, 2025. 2